Original Article

Effects of different dosages esketamine on cardiac conduction and heterogeneity of Cx43: the epicardial mapping in guinea pigs

Ying Cao[1,2#^], Yingnan Song[3#], Zijun Wang[2^], Jian Tang[4], Jing Yi[1,5], Yanqiu Liu[6], Li An[1,5], Zhijun Pan[1,2], Hong Gao[5^]

[1]School of Clinical Medicine, Guizhou Medical University, Guiyang, China; [2]Department of Anesthesiology, The Affiliated Jinyang Hospital of Guizhou Medical University, The Second People's Hospital of Guiyang, Guiyang, China; [3]Translational Medicine Research Center of Guizhou Medical University, Guiyang, China; [4]Department of Anesthesiology, The First People's Hospital of Guizhou University of Traditional Chinese Medicine, Guiyang, China; [5]Department of Anesthesiology, The Affiliated Hospital of Guizhou Medical University, Guiyang, China; [6]Department of Anesthesiology, The Fourth People's Hospital of Guiyang, Guiyang, China

Contributions: (I) Conception and design: Y Cao, Y Song, H Gao; (II) Administrative support: H Gao, Y Liu; (III) Provision of study materials or patients: Y Cao, Y Song, L An, Z Pan; (IV) Collection and assembly of data: Y Cao, Y Song; (V) Data analysis and interpretation: J Tang, J Yi, Z Wang; (VI) Manuscript writing: All authors; (VII) Final approval of manuscript: All authors.

[#]These authors contributed equally to this work.

Correspondence to: Dr. Hong Gao. Department of Anesthesiology, The Affiliated Hospital of Guizhou Medical University, Guiyang, China. Email: 2169617@qq.com; anesth@qq.com.

Background: Esketamine is favored in clinical settings. Relative to other anesthetics it preserves protective airway reflexes, maintains spontaneous respiration, stabilizes hemodynamics, and alleviates neuropathic pain. This study sought to evaluate the cardiac safety of esketamine at 3 sub-anesthetic gradient concentrations.

Methods: We examined the cardiac electrophysiological effects of esketamine with infusion rates of 0.125, 0.25, and 0.5 $mg \cdot kg^{-1} \cdot h^{-1}$. Short-term studies were performed in ventricular myocytes using patch-clamp techniques and optically mapped Langendorff-perfused guinea-pig hearts. Long-term studies were performed using Langendorff-perfused guinea-pig hearts and electrically mapping the receipt of the infusion for 3 hours.

Results: Esketamine changed the action potential (AP) morphology of cardiomyocytes. Notably, it increased the resting membrane potential (RMP), attenuated the amplitude of action potential (APA), reduced the maximum upstroke velocity (Vmax), and shortened the action potential duration (APD) at 30% to 70%, which led to relatively prolonged monophasic action potentials (MAP) triangulation in $G_{0.25}$ and $G_{0.5}$. All the effects were partially eluted. Optical mapping demonstrated almost equal and heterogeneous conduction. $G_{0.125}$ resulted in an increased heart rate (HR) accompanied by a shortened APD. No detectable arrhythmia was observed at the cycle lengths (CLs) used. Long-term electrical mapping demonstrated the dose-dependent deceleration of the Vmax and APA, but only prolonged the AP parameters in $G_{0.5}$. Left-ventricular isochronal conduction maps revealed the conduction heterogeneities at $G_{0.5}$, and conduction velocity (CV) was increased in $G_{0.125}$ and $G_{0.25}$. None of these effects were reversed on drug washout. Electrocardiogram (ECG) traces revealed an accelerated HR with the associated curtailment of QT intervals in $G_{0.125}$; HRs were decreased in $G_{0.25}$ and $G_{0.5}$; the PR intervals and QRS duration differed between $G_{0.125}$ and $G_{0.25}$, $G_{0.5}$, which elicited electrical alternans. Connexin43 (Cx43) expression were significantly decreased in $G_{0.125}$, $G_{0.25}$ and $G_{0.5}$.

Conclusions: These data provide a basic electrophysiology for esketamine. Specifically, we found that (I) various methods of esketamine infusion had different effects on cardiac conduction at different dosages; (II) the heterogeneous expression of Cx43 is associated with spatially dispersed conduction; and (III) potential

^ ORCID: Hong Gao, 0000-0002-3555-5570; Ying Cao, 0000-0003-0699-1039; Zijun Wang, 0000-0002-0532-8940.

cardiac risks should be considered for high-risk patients receiving continuous esketamine infusions of high dosages.

Keywords: Esketamine; cardiac safety; optical mapping; electrical mapping; Connexin43 (Cx43)

Submitted Apr 07, 2022. Accepted for publication Jul 01, 2022.
doi: 10.21037/atm-22-2614
View this article at: https://dx.doi.org/10.21037/atm-22-2614

Introduction

Under the concept of "Rational Perioperative Opioid Management," multi-mode analgesia is becoming more and more important. Ketamine is a racemic mixture in 1:1 of R-ketamine and S-ketamine, and acts as an antagonist of the non-competitive N-methyl-D-aspartate (NMDA)-receptor, which has dissociative anesthetic and analgesic properties (1). Due to the ketamine-induced increase in sympathetic tone, it is a good field anesthetic, as its rapid action and does not cause hypotension or respiratory depression. Historically, the use of ketamine has been limited due to concerns related to its associated psychomimetic effects; it places patients in a state of consciousness to which they are not previously accustomed. Recently, ketamine and esketamine were approved by the Food and Drug Administration as antidepressants for treatment-resistant bipolar depression patients (2). Both ketamine and esketamine have shown gradually recovered in perioperative acute pain management and multimodal analgesia (3).

Esketamine is favored in clinical settings. Relative to other anesthetics, it preserves protective airway reflexes, maintains spontaneous respiration, stabilizes hemodynamics, and alleviates neuropathic pain. The best studied administration route of ketamine is intravenous. Ketamine is a valuable adjunct in the induction and maintenance of anesthesia in patients with unstable hemodynamics and significant pulmonary comorbidities. It can be used as both a sedative and analgesic agent without compromising a patient's respiratory status. In relation to Esketamine's new introductions, such as the antidepressant effects, the reducing suicide ideations and the reduction of dose-dependent dissociative properties of ketamine, safety concerns arise in a number of patient populations, particularly those with widely prevalent comorbidities, like morbid obesity, diabetes mellitus, cardiovascular diseases (e.g., hypertension, cardiac insufficiency, myocardial infarction, and cardiac arrhythmias) and depression-associated comorbidities (e.g., epilepsy and stroke). Safety concerns also arise in relation to concomitant medications, the aging population, and possible adverse reactions from the administered therapies.

In the clinical setting, ketamine acts both directly on cardiac action and activates the autonomic nervous system, which leads to the complex hemodynamic effects. Ketamine has also been shown to produce direct negative inotropic outcomes in heart preparations (4), isolated hearts (5), intact animals (6), or in the clinical trials (7). Ketamine concentration dependently lengthened the RR interval, slowed ventricular conduction velocity (CV), and stretched the period of ventricular effective refractory without induced arrhythmia (8); however, there have been a report of transient bradycardia and hypotension associated with the rapid administration of ketamine at an analgesic dose (9). In guinea-pig myocardium, clinically relevant concentrations of ketamine decreased ischemia-induced action potential (AP) shortening and spontaneous reperfusion-induced ventricular arrhythmias (10). Changes in both CV and refractoriness have been shown to promote arrhythmias of the re-entrant mechanism (11). It has been reported that NMDA-receptor activation induces ventricular electric remodeling and facilitates ventricular arrhythmias (12), reduces heart rate variability (HRV) and enhances atrial fibrillation (AF) inducibility by degrading gap junction proteins (13). Research has examined whether esketamine affects contractility (4-6); however, its electrophysiologic effects on ventricles have only been poorly documented (8). Thus, we conducted the present study first to examine the effects of esketamine on cardiac conduction and susceptibility to arrhythmia, and second to preliminarily explore the potential molecular mechanisms by observing the expression level and distribution of Cx43. We present the following article in accordance with the ARRIVE reporting checklist (available at https://atm.amegroups.com/article/view/10.21037/atm-22-2614/rc).

Methods

Ethical approval

All the procedures were approved by the Institutional Animals Ethics Committee of The Third Affiliated Hospital, Guizhou Medical University (No. 2021A010), Guizhou, China, and conducted according to the national guidelines under which the institution operates, and the National Institutes of Health (NIH) Guidelines for the Care and Use of Laboratory Animals (8th edition). A study protocol was prepared before the study without registration.

Animals

Male guinea pigs (weighing 250–320 g) were purchased from The Experimental Animal Center of Guizhou Medical University. The guinea pigs were housed at 23 ℃ and 60% humidity on a 12/12 h light/dark cycle with free access to chow and water.

Single-cell electrophysiological recordings

Single ventricular myocytes were enzymatically dissociated from the hearts of the adult guinea pigs as described previously (14). In short, the hearts were perfused with Tyrode's solution (containing 5.4 mM of KCl, 135 mM of NaCl, 10 mM of HEPES, 0.33 mM of NaH_2PO_4, 10 mM of glucose, 1 mM of $MgCl_2$, 1.8 mM of $CaCl_2$, and pH 7.4 with NaOH) for 5 min retrogradely to pump out the residual blood. After 5 min of Ca^{2+}-free modified Tyrode's solution perfusion, the solution was switched to 1 containing bovine serum albumin (BSA) fraction (1 mg/mL, Sigma) and collagenase type II (0.52 mg/mL, Worthington Biochemical Corporation), and the hearts were removed from the perfusion apparatus after 40 min. Myocytes were obtained from the free transmural left-ventricular (LV) wall. The myocytes were kept in a KB solution, which was composed of 120 mM of KOH, 120 mM of L-glutamic acid, 10 mM of KCl, 10 mM of Taurine, 10 mM of KH_2PO_4, 10 mM of HEPES, 10 mM of glucose, 0.5 mM of K-EGTA, 0.5 mM of EGTA, 1.8 mM of $MgSO_4{\cdot}7H_2O$, 0.2% BSA, and pH 7.4 with KOH. The cells were then calcified to 1.8 mM and underwent electrophysiological recordings within 6–8 h of isolation. A MultiClamp 700A amplifier, 1550A digitizer, and pCLAMP 10.6 software (Molecular devices, USA) were used to record the APs. The pipette solution contained 130 mM of KCl, 10 mM of NaCl, 0.5 mM of $MgCl_2$, 5 mM of Mg-ATP, 0.5 mM of EGTA, 10 mM of HEPES, 0.4 mM of Tris GTP, and pH 7.2 with KOH. The external solution contained 135 mM of NaCl, 5.4 mM of KCl, 10 mM of HEPES, 0.33 mM of NaH_2PO_4, 10 mM of glucose, 1.8 mM of $CaCl_2$, 1 mM of $MgCl_2$, and pH 7.4 with NaOH. Patch electrodes were pulled with resistances of 3–5 MΩ using a P-97 micropipette puller (Sutter Instruments, USA). The APs were evoked in the current-clamp mode at a rate of 1 Hz with an amplitude of 1,000–3,000 pA current pulse for a duration of 2 ms applied via patch electrodes. The collected data were analyzed using Clampfit software (Version 10, Molecular Devices, USA).

Langendorff-perfused isolated hearts

The guinea pigs (male, weighing 250–320 g) were humanely sacrificed by inhaling 8% sevoflurane vaporized with 60% oxygen. After thoracotomy, the hearts were rapidly excised and then mounted onto a Langendorff-perfusion system, after which they were perfused with the modified Tyrode's solution (containing 119 mM of NaCl, 4 mM of KCl, 1 mM of $MgCl_2{\cdot}6$ mM of H_2O, 25 mM of $NaHCO_3$, 1.2 mM of KH_2PO_4, 1.8 mM of $CaCl_2$, and 10 mM of glucose), equilibrated with 95% O_2–5% CO_2, pH =7.35~7.45, at a flow rate of 8 mL/min at 37 ℃. The hearts were monitored and sustained for 20 min before the experimental procedures commenced.

Ex-vivo heart preparations for optical mapping

After the Langendorff-perfused hearts reached stability, the contraction artefacts were minimized using 10 μM of blebbistatin (Tocris Bioscience, MN, USA). Dye loading was aided by pre-perfusion with pluronic F127 (20% w/v in DMSO). Rh237 (V_m indicator) and Rhod2-AM (Ca_i indicator) were perfused to enable the measurement of the simultaneous membrane potential and Ca^{2+} at 37 ℃. Epifuorescence was acquired simultaneously using high-speed cameras (Integrated Imaging Systems; Cairn Research, Kent, England). Action potential duration at 90% (APD_{90}) repolarization and CV were studied using a dynamic pacing protocol. Ventricular tachyarrhythmias (VTA) inducibility was defined as the ability to provoke Ventricular Tachycardia/Ventricular Fibrillation (VT/VF) with the dynamic pacing protocol and/or programmed extra-stimuli. To analyze the optical mapping signals and generate the isochronal maps, the data were semi-automatically processed using ElectroMap software.

Stimulation protocol

The S_1S_2 protocol was used to assess arrhythmogenicity and identify re-entrant substrates (15). The electrical recordings were made during programmed stimulations that involved the application of the premature extra-stimulus (S_2) after a train of 7 regular (S_1) pulses. The protocol was performed both before and after the drugs were delivered. The stimuli were generated by an isolated constant voltage/current stimulator (MyoPacer EP Field Stimulator, IonOptix, Milton, MA, USA), and delivered onto the epicardial apex at a 2 ms pulse width and an amplitude 1.5× the diastolic voltage threshold with a platinum electrode. The heart was paced at basic cycle lengths (BCL) from 200 to 170 ms with consecutive 10 ms decrements of 2 ms in duration for 50 times. The optical mapping recording was performed at the last 2 s in each episode.

Ex-vivo heart preparations for electrical mapping

The guinea-pig hearts were randomly divided into 4 groups (n=6 per group). The control group ($G_{control}$) did not receive esketamine (No. 210425BL, Jiangsu Hengrui Pharmaceutical Co., Jiangsu, China). In the remaining 3 groups, the hearts were treated with the following different doses: 0.125 $mg{\cdot}kg^{-1}{\cdot}h^{-1}$ (the 0.125 group or $G_{0.125}$), 0.25 $mg{\cdot}kg^{-1}{\cdot}h^{-1}$ (the 0.25 group or $G_{0.25}$), and 0.5 $mg{\cdot}kg^{-1}{\cdot}h^{-1}$ (the 0.5 group or $G_{0.5}$). The drugs were administered with Tyrode's solution. After their successful preparation, the hearts were perfused on the Langendorff apparatus. Immediately after stabilization, the experimental protocol of continuous perfusion for 3 h was commenced. Electrocardiograms (ECGs) were continuously recorded by 2 ECG electrodes (IH-SR, Hugo Sachs Elektronic, GER), positioned on the right atrium and left ventricle, respectively. A 64-channel multi-electrical array (MEA) mapping system (EMS64-USB-1003, MappingLab Ltd., UK) was employed to record the extracellular potential of the LV epicardium. EMapRecord 5.0 software (MappingLab Ltd., UK) was used to monitor and calculate the CV from the known distance between the recording points and the difference in timing. The data were stored for the subsequent off-line analysis.

Western blot and immunofluorescence detection

Western blot

The expressions of the Cx43 proteins in each group were detected by Western blot. Cardiac tissues were dissected from the left ventricle at the end of the *ex-vivo* electrophysiological studies for protein quantification (n=6 per group). The ventricle myocardium tissues were homogenized after 200 μL of the specific cocktail proportion of proteinlysate and protease inhibitor were added at 4 ℃ and centrifuged at 12,000 rpm for 15 min. The sample proteins were quantified by BCA colorimetric assays, and phosphate buffered solution (PBS) was then used to dilute the samples to the same concentration. The samples were boiled at 100 ℃ for 10 min, and 12% separating gel and 5% loading gel were used for separating by sodium dodecyl-sulfate polyacrylamide gel electrophoresis. Electrophoresis was performed in the electrophoretic buffer, and the target bands were then then transferred to polyvinylidene fluoride membranes by semi-dry transfer (10V, 15 min). The membranes were blocked with 5% BSA and incubated in tris buffered saline with tween (TBST) for 2 hours. They were washed with TBST and incubated overnight with the following primary antibodies at 4 ℃: anti-connexin 43 antibody (1:1,000, Sigma, USA) and anti-GAPDH antibody (1:500, Abcam, Cambridge, UK). The next day, after washing with TBST, the membranes were incubated at room temperature for 1 hour with a second antibody (rabbit anti-goat, 1:12,000, Beijing Boosen Biotechnology Co., Ltd., Beijing, China), which was labeled with horseradish peroxidase. They were then washed with TBST again, and ECL hypersensitive reagent was added to the membranes. Next, an automatic gel imaging analysis system was used to visualize (ZF-158, American Bio-rad Company).

Single immuno-labeling Cx43 immunofluorescence

The paraffin sections were made to detect Cx43 using immunofluorescence as previously described in detail (16). The apex cordis tissues were fixed, dehydrated, paraffin embedded, and sectioned. Cryostat sections, 8 μm thick, were mounted on glass slides overnight at 40 ℃. Rehydration and heat-induced epitope retrieval were then performed. The sections were subsequently incubated with a goat-anti-rabbit Cx43 (8 h at 4 ℃; 1:2,000, Bioss, Beijing, China). After being washed 3 times in PBS, the sections were incubated with IgG H&L FITC (1:200, Abcam, Cambridge, England). After nuclear staining with DAPI [Mounting Medium, antifading (with DAPI), Solarbio Inc., China], 5 random fields of each slide were separately observed and examined with a microscope illuminated by a sequential scanning mode at 405 and 488 nm (40×, Olympus IX83, Olympus Life Science Inverted Microscopes, Japan),

and the fluorescence intensity was determined using ImageJ software.

Statistical analysis

SPSS 17.0 software was used for the data analysis (SPSS, Chicago, IL, USA). Clampfit 10.6 (Molecular Devices, USA), OriginPro 8.0 (Origin Lab, USA), and Adobe Illustrator 10.0 (Adobe, USA) were used to analyze the patch-clamp recorded data. All the data are expressed as the means ± standard errors of the means. A one-way analysis of variance followed by a multiple-comparison test was used to evaluate the multiple test treatments. A P value <0.05 was considered statistically significant. In the figures, the designations for the P values are as follows: *, P<0.05, **, P<0.01, and ***, P<0.001 respectively.

Results

Patch-clamp studies of single-cell APD

We examined the effects of different doses on the AP parameters in single guinea-pig ventricular myocytes. At a stimulation frequency of 1 Hz, the action potential duration (APD), resting membrane potential (RMP), maximum upstroke velocity (Vmax), amplitude of action potential (APA), and APD at 30%, 50%, 70%, and 90% (APD_{30}, APD_{50}, APD_{70}, APD_{90}) repolarization were recorded via the bath perfusion system. The results showed esketamine changed the AP morphology of the cardiomyocytes (see *Figure 1A*) and increased the RMP of the cardiomyocytes (see *Figure 1B*), attenuated the APA (see *Figure 1C*), reduced the Vmax (see *Figure 1D*) and shortened the APD_{30} ~APD_{70} (see *Figure 1E-1G*) and there are no significant changes between groups in APD_{90} (see *Figure 1H*), which led to no changes in early repolarization phase (see *Figure 1I*) but a relatively prolonged late repolarization phase (see *Figure 1J*) and MAP triangulation in $G_{0.25}$ and $G_{0.5}$ (see *Figure 1K*). All the effects were especially significant in $G_{0.5}$ and were then partially eluted.

Optical mapping studies and assessments of arrhythmic tendency in ex-vivo heart preparations

We then investigated the effects of different dosages of esketamine with continuous intravenous infusion optical fluorescence mapping in sinus-paced Langendorff-perfused hearts using the recording and ECG monitoring configurations (see *Figure 2A*). AP initiation and conduction were measured by voltage mapping (see *Figure 2B*), and we found an increase in HR in $G_{0.125}$, but a decrease in HR in $G_{0.25}$ and $G_{0.5}$ [see *Figure 2B* (i and iii)] with more heterogeneous and almost equal conduction [see *Figure 2B* (iv)]. Additionally, optical potentiometric mapping revealed that $G_{0.125}$ shortened APD_{90} [see *Figure 2B* (ii and v)]. Finally, voltage dye optical mapping studies during ventricular pacing were used to assess susceptibility of the isolated perfused hearts to the induction of arrhythmias before and after drug administration [see *Figure 2C* (ii)], but no arrhythmic effects were detected at the CLs used.

Ex-vivo heart preparations of electrical mapping and electrocardiographic studies

Next, we explored the long-term effects of 3 different dosages of esketamine in whole isolated hearts with continuous infusion on electrophysiological activation and recovery. *Figure 3A* summarizes the sites of the ECG and MEA recordings in the electrical mapping. *Figure 3B* shows that the APs recorded from the defined LV [see *Figure 3B* (ii and iii)] in the presence of esketamine. LV isochronal conduction maps [see *Figure 3C* (i)] were observed in the presence of esketamine revealed there was no significant difference in RMP between groups [see *Figure 3C* (ii)], a synergistic reduction of the APA [see *Figure 3C* (iii)], and a clear dose-depended deceleration of the Vmax [see *Figure 3C* (iv)]. Compared with $G_{control}$, APD_{30} was increased from $G_{0.125}$ to $G_{0.5}$ [see *Figure 3C* (v)]; APD_{50}, APD_{70} and especially APD_{90} of $G_{0.125}$ were decreased, the parameters of $G_{0.25}$ were basically the same as those of the $G_{control}$; every stage in $G_{0.5}$ were significantly increased which resulted the APD was only prolonged in $G_{0.5}$ [see *Figure 3C* (vi-ix)]; Compared with $G_{control}$, APD_{30-60} [see *Figure 3C* (x)] was significantly shortened. there was no significant difference between each group in APD_{60-90} [see *Figure 3C* (xi)] and also APD_{30-90} was significantly shortened in $G_{0.125}$ and $G_{0.25}$ [see *Figure 3C* (xii)]. Compared with $G_{0.125}$ and $G_{0.25}$, APD_{30-60} [see *Figure 3C* (x)] and APD_{30-90} [see *Figure 3C* (xii)] were significantly prolonged in $G_{0.5}$. Notably, there were conduction heterogeneities in $G_{0.5}$, and the CV was markedly increased in $G_{0.125}$ and $G_{0.25}$ [see *Figure 3C* (i)]. These effects were not all reversed on drug washout. The quantification of the corresponding ECG traces [see *Figure 3D* (i–iv)] showed that $G_{0.125}$ accelerated the HR [see *Figure 3D* (i) and *Figure 3E* (i)] with an associated curtailment of the QT intervals [see *Figure 3E* (ii)], but both $G_{0.25}$ and $G_{0.5}$ exhibited the opposite effects. The PR interval

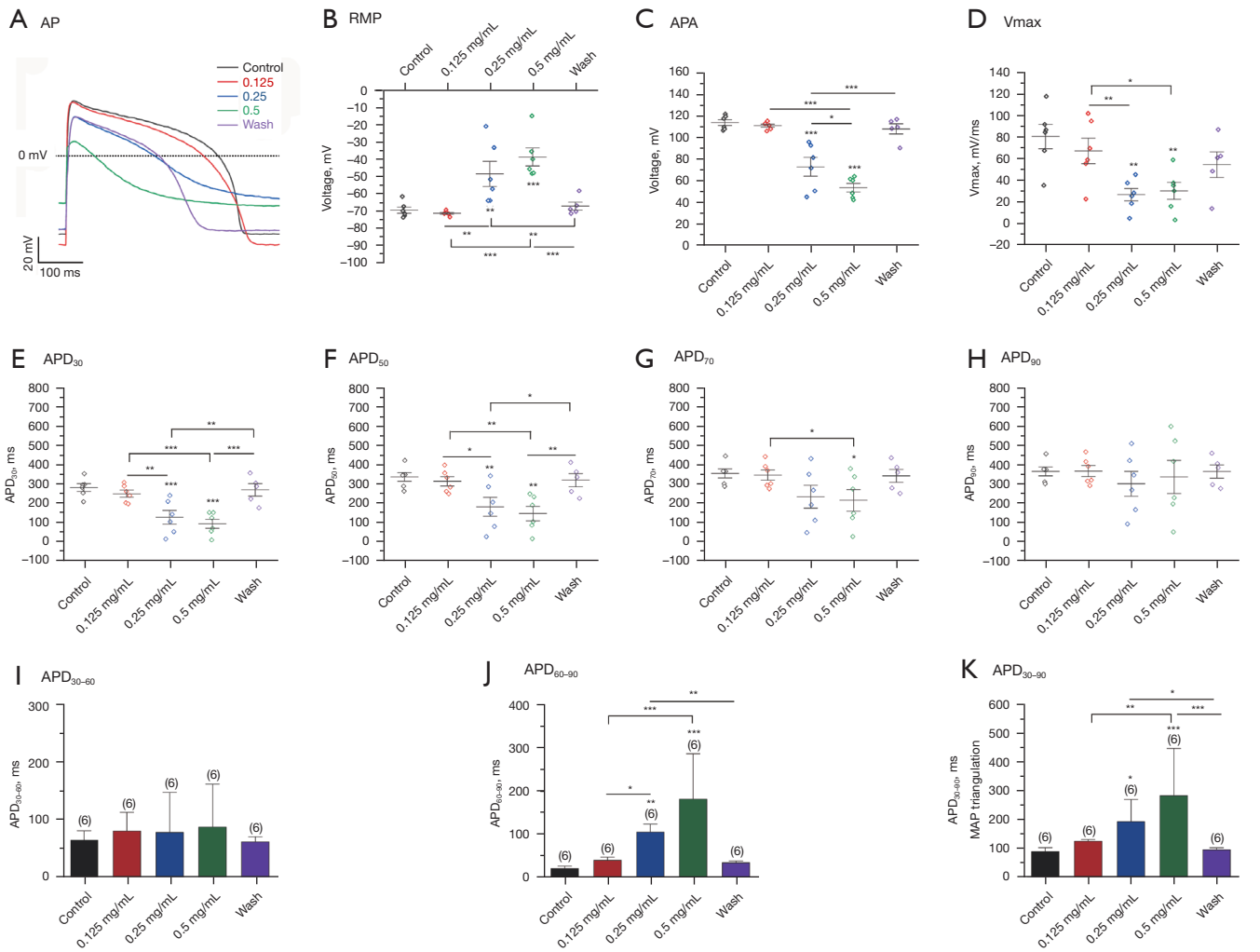

Figure 1 Effects of different dosages of esketamine on the AP in single guinea-pig ventricular myocytes. (A) APs recorded; (B-H) corresponding measured (B) RMP, (C) APA, (D) Vmax, (E) APD_{30}, (F) APD_{50}, (G) APD_{70}, (H) APD_{90}; (I) $APD_{30–60}$, (J) $APD_{60–90}$ and (K) MAP triangulation ($APD_{30–90}$). (Six cardiocytes per group; *, P<0.05, **, P<0.01 and ***, P<0.001). AP, action potential; RMP, resting membrane potential; APA, amplitude of action potential; APD_{30}, action potential duration at 30%; APD_{50}, action potential duration at 50%; APD_{70}, action potential duration at 70%; APD_{90}, action potential duration at 90%; $APD_{30–60}$, action potential duration from 30% to 60%; $APD_{60–90}$, action potential duration from 60% to 90%; $APD_{30–90}$, action potential duration from 30% to 90%; MAP, monophasic action potentials.

[see *Figure 3E* (iii)], and the QRS durations [see *Figure 3E* (iv)] differed significantly between $G_{0.125}$ and $G_{0.25}$, $G_{0.5}$, which elicited electrical alternans. Together, these results suggested that $G_{0.5}$ exerted an inhibitory effect on the HR and CV, and prolonged cardiac repolarization.

Immunofluorescence detection and Western blot

The expression of Cx43 in the left ventricle was detected by immunofluorescence [see *Figure 4A* (i)], compared to the $G_{control}$, the fluorescence intensity of Cx43 was meaningfully declined in $G_{0.125}$, $G_{0.25}$, and $G_{0.5}$ [see *Figure 4A* (ii)]. The quantified expression of Cx43 detected by western blot [see *Figure 4B* (i)] is consistent with the IF [see *Figure 4B* (ii)].

Discussion

The main and original results of the present study are as follows: (I) no arrhythmogenesis spontaneously occurred during and after the clinically relevant concentrations

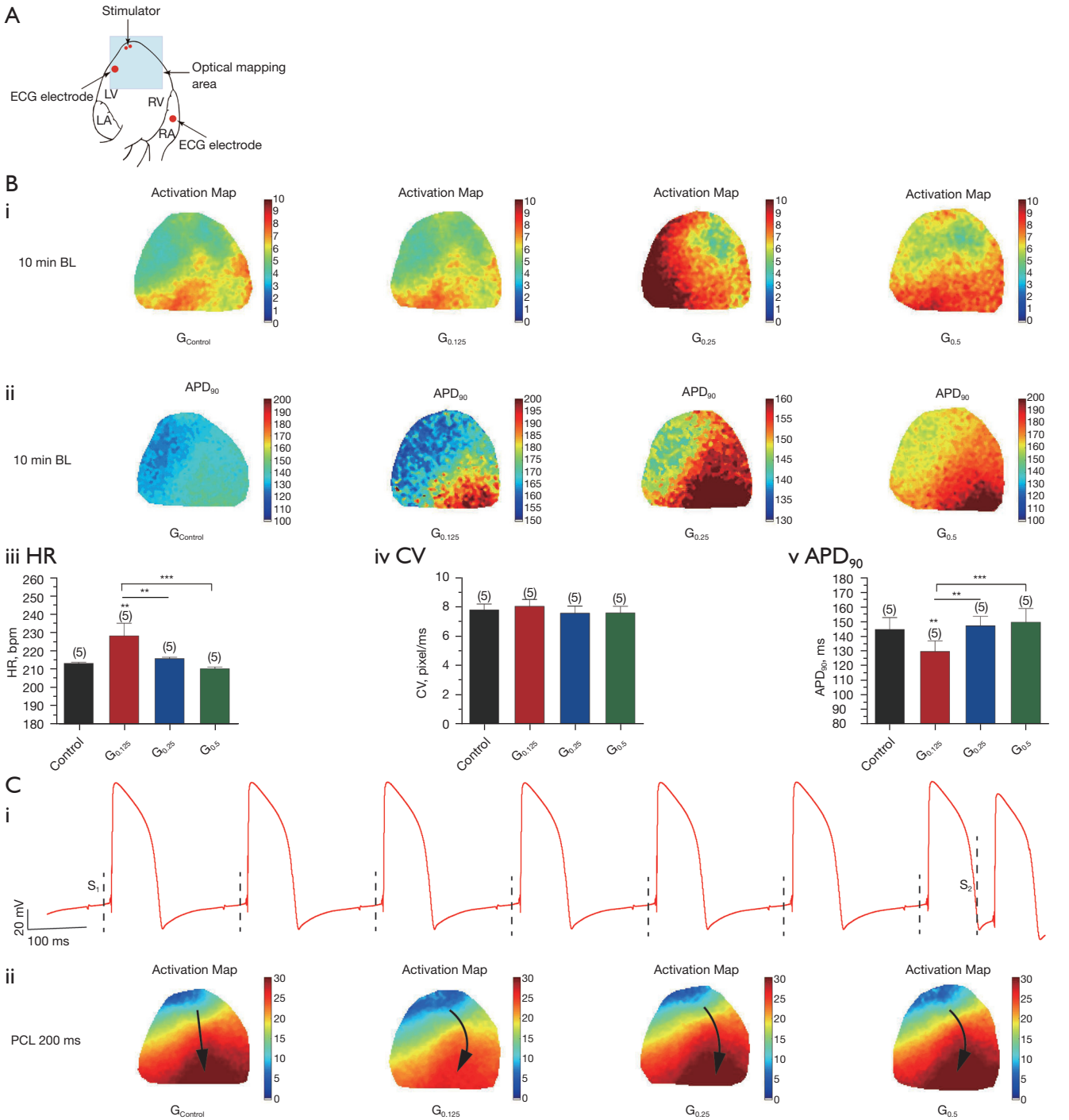

Figure 2 Optical mapping of voltage RH237 and Rhod-2 in isolated Langendorff-perfused hearts. (A) ECG monitoring and optical mapping configuration; (B) (i) AP initiation mapping, (ii) maps of APD_{90}; corresponding measured, (iii) HR, (iv) conduction, and (v) APD_{90} averaged over the field of view velocities; (C) (i) a premature AP was induced on extra-stimulus application S_2 immediately after termination of the effective refractory period in the preceding S_1 beat; the upper and the lower MAP were recorded, respectively, and (ii) voltage RH237 optical mapping of ventricular arrhythmic tendency in isolated Langendorff-perfused hearts. (This procedure was repeated on 5 hearts; **, P<0.01 and ***, P<0.001). ECG, electrocardiogram; AP, action potential; HR, heart rate; CV, conduction velocity; APD_{90}, action potential duration at 90%; LV, left ventricle; RV, right ventricle; LA, left atrium; RA, right atrium; BL, base line; PCL, pacing cycle lengths.

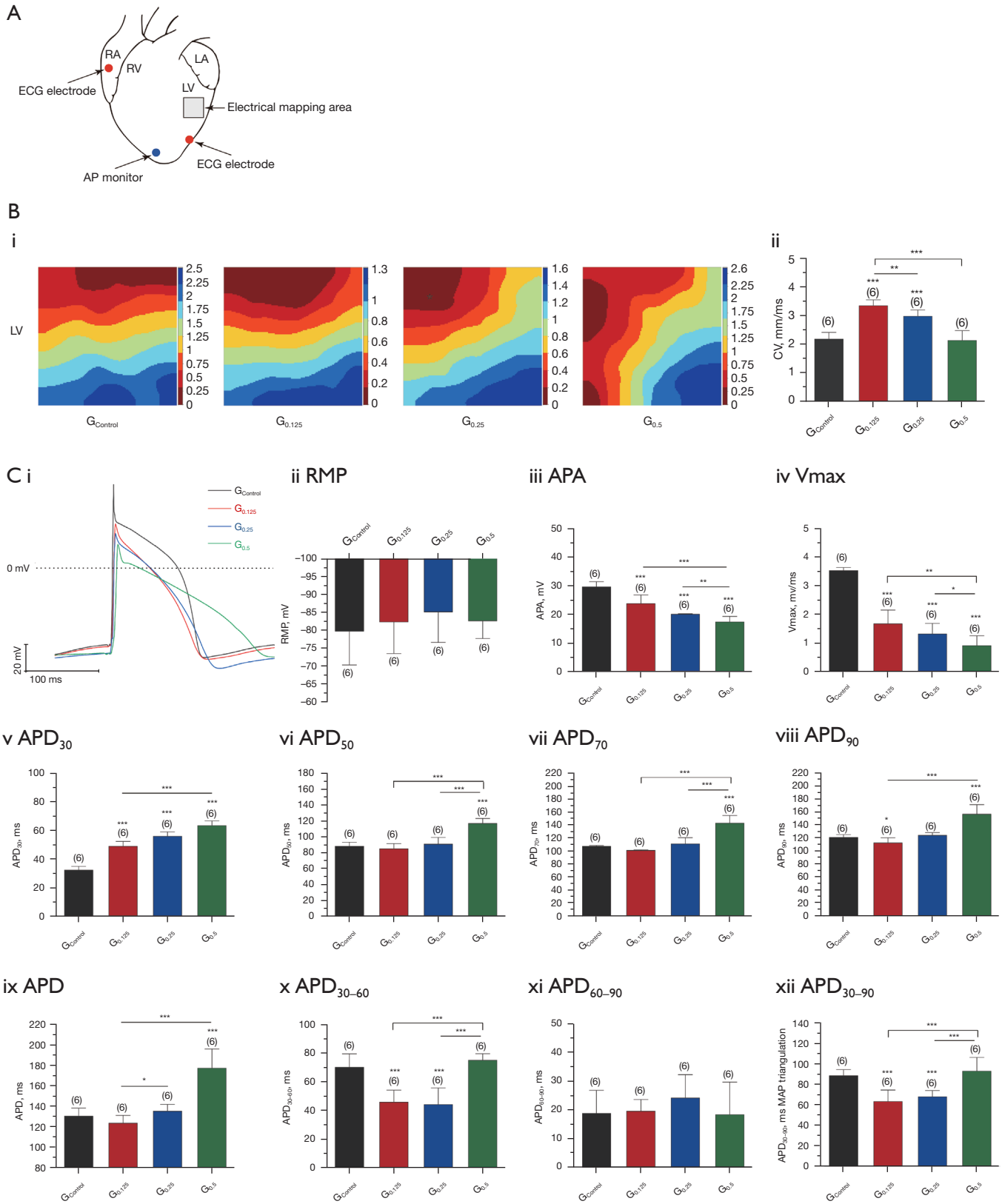

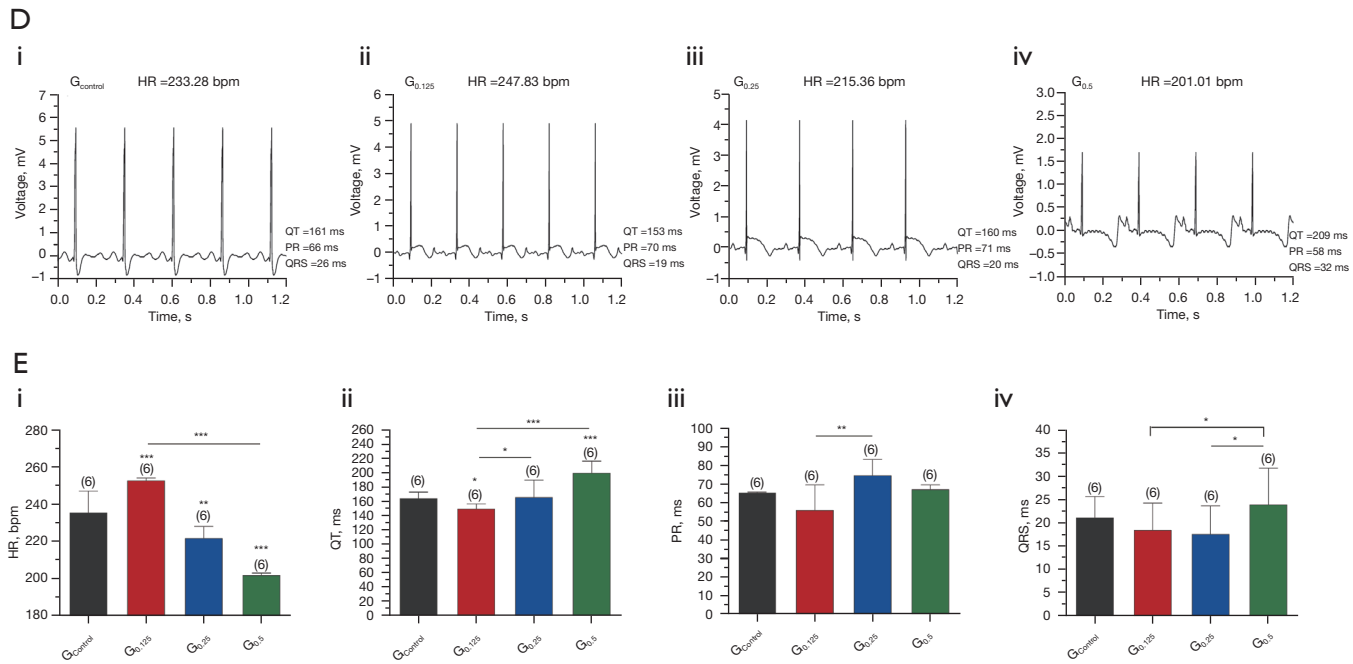

Figure 3 MEA mapping and ECG studies in isolated Langendorff-perfused guinea-pig hearts following continuous perfusion for 3 h. (A) Schematic summary of MEA and ECG recording configuration; (B) (i) successive LV isochronal maps, and (ii) quantified conduction velocities for the conditions; (C) (i) representative APs recorded from the defined LV, (ii) RMP, (iii) APA, (iv) Vmax, (v) APD_{30}, (vi) APD_{50}, (vii) APD_{70}, (viii) APD_{90}, (ix) APD, (x) $APD_{30–60}$, (xi) $APD_{60–90}$ and (xii) $APD_{30–90}$, MAP triangulation; (D) ECG studies, ECG records obtained as described above, followed by drug washout, (i) $G_{control}$, (ii) $G_{0.125}$, (iii) $G_{0.25}$ and (iv) $G_{0.5}$; (E) ECG corresponding measured (i) HR, (ii) QT intervals, (iii) PR intervals and (iv) QRS durations. (Six hearts per group; *, P<0.05, **, P<0.01 and ***, P<0.001). MEA, multi-electrical array; ECG, electrocardiogram; AP, action potential; RMP, resting membrane potential; APA, amplitude of action potential; APD, action potential duration; APD_{30}, action potential duration at 30%; APD_{50}, action potential duration at 50%; APD_{70}, action potential duration at 70%; APD_{90}, action potential duration at 90%; $APD_{30–60}$, action potential duration from 30% to 60%; $APD_{60–90}$, action potential duration from 60% to 90%; $APD_{30–90}$, action potential duration from 30% to 90%; LV, left ventricle; HR, heart rate; RV, right ventricle; LA, left atrium; RA, right atrium.

of esketamine were administered; (II) arrhythmia could not be induced by pacing; (III) the prolonged infusion of high dosages of esketamine altered the cardiac electrophysiological effects and caused visible conduction heterogeneities; and (IV) heterogeneous Cx43 expression is associated with spatially dispersed conduction.

The use of opioids for analgesia might cause hyperalgesia and patients can develop a tolerance to opioids, both of which are partially attributed to NMDA-receptor activation. Preventive and post-operative analgesia with NMDAR antagonists can block the acute tolerance of opioids and reduce the development of neuropathic pain (17). A study had reported that a low-dose intravenous infusion of ketamine can be used in acute and chronic post-operative pain management (18). Despite these advantages, the side effects of ketamine, which include nightmares and delusions, limit its routine use. However, some research has suggested that the acute psychoactive effects, including the dissociative, psychotomimetic, and 'mystical' effects, experienced during or shortly after a sub-anesthetic dosage of ketamine administration, may be associated with its therapeutic benefits. Esketamine has twice the analgesic effect of racemic ketamine, has fewer side effects, such as hallucinations, results in a faster recovery, and is able to lower the sevoflurane MAC value (19). Esketamine also has sympathomimetic properties that cause less cardiorespiratory depression than other sedatives, which had been reported that propofol combined with esketamine exhibited a good safety profile and high reliability, was more conducive to the hemodynamics stability, alleviating surgical

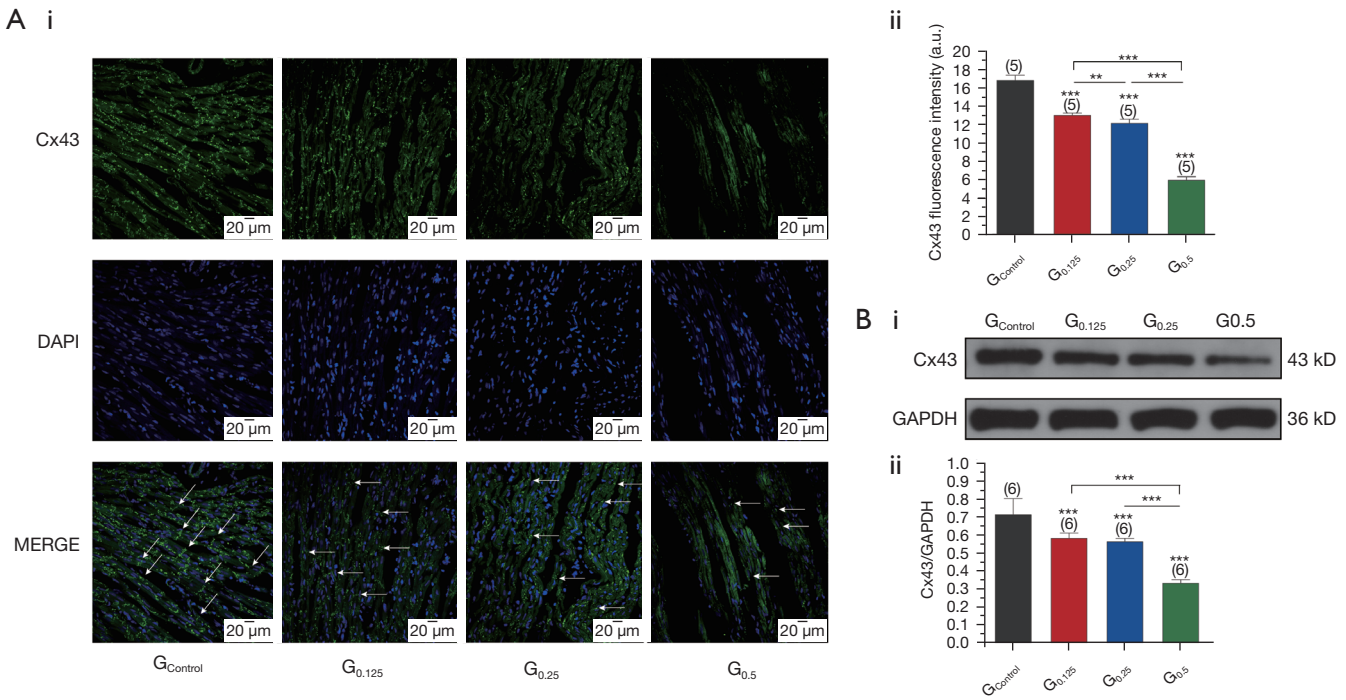

Figure 4 Immunofluorescence and confocal laser scanning microscopy of Cx43 (A), localization (arrows) at the membrane of neighboring cells [detail A (i), and merged image]. High-intensity specific immunoreactive signals of Cx43 were clearly identified and regularly distributed in $G_{control}$ compared to the other groups; with the duration of continuous infusion Cx43 signals decreased and were heterogeneously distributed A (ii). The expression levels of Cx43 were examined by Western blot (B). Cx43 expression were significantly decreased in $G_{0.125}$, $G_{0.25}$ and $G_{0.5}$, compared with $G_{0.125}$ and $G_{0.25}$, $G_{0.5}$ was significantly decreased. (Six hearts per group; **, P<0.01 and ***, P<0.001).

stress and inflammatory responses (20). Theoretically, esketamine possesses some non-opioid analgesic properties that aim to reduce opioids consumption among patients undergoing surgery, improve recovery, and alleviate opioid-related side effects; it had been reported that esketamine effectively countered remifentanil-induced respiratory depression which attributed to an increase in remifentanil-reduced ventilatory CO_2 chemosensitivity (21). Thus, the use of esketamine in perioperative pain management is promising.

Despite its wide clinical use in perioperative patients, minimal data indicate that single doses of intravenous esketamine or ketamine use during cesarean section delivery may not affect the breastfed infant or lactation (22), and no instances of clinically apparent liver injury have as yet been reported with long term use of esketamine (23). There also has very few studies examined the effects of esketamine on cardiac electrophysiology. Based on drug instructions and reference materials, the required dosages of esketamine are usually 0.1–0.5 $mg \cdot kg^{-1} \cdot h^{-1}$(approximate mean: 0.4 $mg \cdot kg^{-1} \cdot h^{-1}$) (24,25) with or without bolus. It has been reported that in most critically ill patients suffering from COVID-19 induced acute respiratory distress syndrome (ARDS), the prescribed sedation levels are only achievable with several combinations of sedatives, and a mean dose of 0.86 (±0.76) $mg \cdot kg^{-1} \cdot h^{-1}$ of esketamine as an NMDAR inhibitor was required (26). In our study, we examined 1 control group and 3 dosing groups (i.e., $G_{0.125}$, $G_{0.25}$, and $G_{0.5}$) that received continuous intravenous doses at wide concentration ranges that encompassed the reported therapeutic levels.

The cardiac AP arises and spreads throughout the myocardium as a consequence of the highly organized spatial and temporal expression of ion channels conducting Na^+, Ca^{2+} or K^+ currents, which when changed, may induce cardiac arrhythmias. The effects of a drug on the AP parameters can predict its effects on each ion current. In this study, we first investigated the electrophysiology of esketamine on APs in the ventricular myocytes of guinea pigs. Similar to previous studies on ketamine, we found

that esketamine produced decreases in the Vmax, APA, and APD_{50}, and increases in the RMP and APD_{90}, which indicated that it exerted a frequency-independent inhibitory action on the cardiac fast inward sodium current (I_{Na}) (27,28) in $G_{0.25}$ and $G_{0.5}$. As inward rectifier potassium currents (I_{K1}) maintain RMP and modulate the phase-3 repolarization of the APD in cardiomyocytes (29,30), the short-term cellular electrophysiological assays with the plateau of the RMP shifted to more positive values. However, RMP was not observed to change in isolated hearts. This may be because drugs are more highly dispersed in individual cells than dense tissues.

Additionally, the effects of esketamine on AP repolarization were somewhat complicated, and depended on the infusion rate and treatment period. In the *in-vitro* cell experiments, the APD_{30} and the APD_{50} decreased in $G_{0.25}$ and $G_{0.5}$, which accelerated the repolarization, while the APD_{70} gradually recovered in $G_{0.125}$, and the APD_{90} changed insignificantly in all groups. Optical mapping perfuses with voltage-sensitive dyes and either biochemical or mechanical contractile uncoupling, which may also interfere with the wave shape of normal APs (31). We found that only the APD_{90} decreased in $G_{0.125}$. Next, we found that in the isolated hearts with long-term esketamine continual perfusion, the APD_{30} was prolonged in all treatment groups. With higher concentrations and longer exposure times, the APD_{90} was obviously prolonged in $G_{0.5}$ and shortened in $G_{0.125}$. Our previous studies have also demonstrated that dexmedetomidine can prolong APD_{50} and APD_{90} which maybe the mechanism of slowing HR (32), and sevoflurane alleviates reperfusion arrhythmia induced by myocardial ischemia-reperfusion through the shortening of $MAPD_{90}$ in isolated rat hearts (33).

There are reports that some drugs barely affect the APD_{90} in isolated guinea-pig papillary muscles (4,5), but prolong the QT intervals in humans (34), which indicate that the APD_{90} alone is not reliable for evaluating the inhibitory effects of compounds on ion currents. MAP triangulation, which is defined as the slowing of final repolarization, has been shown to be a strong predictor of early afterdepolarizations (EADs) or proarrhythmia. The cell study showed the plateau drooped, which resulted in the AP becoming more triangular. Additionally, the APD_{30} shortened, and the largest prolongation was limited to the APD_{90}. Conversely, at the level of the whole heart, the final AP was prolonged in the high-dosage group that showed markedly changed the plateau. Generally, a shortened or lengthened APD is only proarrhythmic when combined with instability, triangulation, or reverse use-dependence but can become antiarrhythmic when ≥1 of these are absent. The drug induced the prolongation of APD with a square AP is antiarrhythmic (35).

Notably, repolarization disturbance limitation, abnormal automaticity (36) and conduction disturbances (37) can lead to monomorphic arrhythmias (including VT) (38). Using optical voltage mapping and electrical mapping, we also demonstrated that ventricular conduction in response to esketamine is complicated. As reflected by the prolongation of the QRS duration in $G_{0.5}$ electrocardiographically, the intraventricular conduction was clearly compromised. Additionally, the cardiac conduction heterogeneity increased. Gap junction expression and function can also influence cardiac conduction through ion channel availability (39). The effects of the $G_{0.5}$ sustained infusion are similar to those previously reported for ketamine slowed CV, and prolonged refractoriness without changing anisotropy or increasing dispersion of refractoriness, which resulted in the significant antiarrhythmic effects of ketamine (8).

Cx43 is known to be mainly expressed in ventricular cardiomyocytes. We observed that Cx43 in the membranous fraction was reduced in the treatment groups. Intriguingly, the effects of long-term low- and medium-dosages of esketamine on the CV and ECG parameters were largely opposite to the changes in Cx43 expression. Notably, the level of connexin proteins are related to intercellular coupling through many complicated factors, including trafficking, assembly, and posttranslational modification. It has been reported that the inhibition of cardiac gap junctional communication by the lipophilic drugs (such as heptanol, octanol, oleic acid or palmitoleic acid) is their ability to dissolve in the lipid bilayer that lead to impairment of the transcellular gap junction channels (40,41), which might explained the relevantly effects of esketamine on Cx43 expressions. The heart has a conduction reserve, and a medium and homogeneous decrease of 50% in Cx43 expression by itself does not always lead to conduction impairment (42). The enhanced sympathomimetic activities compatible with the increased vascular contraction and raising HR were common in clinical observations (43) and *in-vivo* studies (44). The Langendorff-perfusion system itself is separate from neural and humoral control. The NMDA-receptor is widely expressed in the heart and is involved in the onset of arrhythmias, and research has shown that its inhibition could improve Cx43 degradation (45). Previous studies have shown that ketamine-induced cardiovascular responses are centrally mediated (46,47). A previous study

showed that ketamine does not produce a pressor response in dogs by epidural anesthesia (48). There are also reports that due to the release of or response to synaptic transmitter substances were more effectively inhibited in sympathetic ganglia than at sympathetic neuromuscular junctions (49), ketamine can potentiate responses to both noradrenaline and sympathetic nerve stimulation *in vitro* (50). These results need to be further explored.

Conclusions

The main and original results from this study are as follows: (I) various methods of esketamine infusion showed a far cry from effects on cardiac conduction with different dosages; and (II) high-risk patients using continuous infusions of high dosages of esketamine should be concerned about potential cardiac risks.

Limitations of the present study

The present study did not explore the association between ion channels, NMDA-receptors, and Cx43. Further, parallel clinical investigations on humans need to be conducted to explore the blood or plasma concentrations which correlated to effective concentration and to corresponding dosages for clinical pharmacokinetic properties of esketamine.

Acknowledgments

Funding: This study was supported by the Science and Technology Fund Project of Guizhou Health Commission in 2021 (HG: gzwkj2021-270, and YC: gzwkj2021-281), and the Traditional Chinese Medicine, Ethnic Medicine Science and Technology Research Special Project of Guizhou Province (HG: QZYY-2021-102, and ZJW: QZYY-2021-134).

Footnote

Reporting Checklist: The authors have completed the ARRIVE reporting checklist. Available at https://atm.amegroups.com/article/view/10.21037/atm-22-2614/rc

Data Sharing Statement: Available at https://atm.amegroups.com/article/view/10.21037/atm-22-2614/dss

Conflicts of Interest: All authors have completed the ICMJE uniform disclosure form (available at https://atm.amegroups.com/article/view/10.21037/atm-22-2614/coif). The authors have no conflicts of interest to declare.

Ethical Statement: The authors are accountable for all aspects of the work in ensuring that questions related to the accuracy or integrity of any part of the work are appropriately investigated and resolved. All the procedures were approved by the Institutional Animals Ethics Committee of The Third Affiliated Hospital, Guizhou Medical University (No. 2021A010), Guizhou, China, and conducted according to the national guidelines under which the institution operates, and the NIH Guidelines for the Care and Use of Laboratory Animals (8th edition).

References

1. Daly EJ, Singh JB, Fedgchin M, et al. Efficacy and Safety of Intranasal Esketamine Adjunctive to Oral Antidepressant Therapy in Treatment-Resistant Depression: A Randomized Clinical Trial. JAMA Psychiatry 2018;75:139-48.
2. Segmiller F, Rüther T, Linhardt A, et al. Repeated S-ketamine infusions in therapy resistant depression: a case series. J Clin Pharmacol 2013;53:996-8.
3. Schwenk ES, Viscusi ER, Buvanendran A, et al. Consensus Guidelines on the Use of Intravenous Ketamine Infusions for Acute Pain Management From the American Society of Regional Anesthesia and Pain Medicine, the American Academy of Pain Medicine, and the American Society of Anesthesiologists. Reg Anesth Pain Med 2018;43:456-66.
4. Endou M, Hattori Y, Nakaya H, et al. Electrophysiologic mechanisms responsible for inotropic responses to ketamine in guinea pig and rat myocardium. Anesthesiology 1992;76:409-18.
5. Graf BM, Vicenzi MN, Martin E, et al. Ketamine has stereospecific effects in the isolated perfused guinea pig heart. Anesthesiology 1995;82:1426-37; discussion 25A.
6. Pagel PS, Schmeling WT, Kampine JP, et al. Alteration

of canine left ventricular diastolic function by intravenous anesthetics in vivo. Ketamine and propofol. Anesthesiology 1992;76:419-25.
7. Suleiman Z, Ik K, Bo B. Evaluation of the cardiovascular stimulation effects after induction of anaesthesia with ketamine. J West Afr Coll Surg 2012;2:38-52.
8. Aya AG, Robert E, Bruelle P, et al. Effects of ketamine on ventricular conduction, refractoriness, and wavelength: potential antiarrhythmic effects: a high-resolution epicardial mapping in rabbit hearts. Anesthesiology 1997;87:1417-27.
9. Emerling AD, Fisher J, Walrath B, et al. Rapid Ketamine Infusion at an Analgesic Dose Resulting in Transient Hypotension and Bradycardia in the Emergency Department. J Spec Oper Med 2020;20:31-3.
10. Hanouz JL, Repesse Y, Zhu L, et al. The electrophysiological effects of racemic ketamine and etomidate in an in vitro model of "border zone" between normal and ischemic/reperfused guinea pig myocardium. Anesth Analg 2008;106:365-70, table of contents.
11. Varró A, Tomek J, Nagy N, et al. Cardiac transmembrane ion channels and action potentials: cellular physiology and arrhythmogenic behavior. Physiol Rev 2021;101:1083-76.
12. Shi S, Liu T, Li Y, et al. Chronic N-methyl-D-aspartate receptor activation induces cardiac electrical remodeling and increases susceptibility to ventricular arrhythmias. Pacing Clin Electrophysiol 2014;37:1367-77.
13. Shi S, Liu T, Wang D, et al. Activation of N-methyl-d-aspartate receptors reduces heart rate variability and facilitates atrial fibrillation in rats. Europace 2017;19:1237-43.
14. Wang YH, Shi CX, Dong F, et al. Inhibition of the rapid component of the delayed rectifier potassium current in ventricular myocytes by angiotensin II via the AT1 receptor. Br J Pharmacol 2008;154:429-39.
15. Tse G, Wong ST, Tse V, et al. Restitution analysis of alternans using dynamic pacing and its comparison with S1S2 restitution in heptanol-treated, hypokalaemic Langendorff-perfused mouse hearts. Biomed Rep 2016;4:673-80.
16. Abu Abed U, Brinkmann V. Immunofluorescence Labelling of Human and Murine Neutrophil Extracellular Traps in Paraffin-Embedded Tissue. J Vis Exp 2019. doi: 10.3791/60115.
17. De Kock M, Lavand'homme P, Waterloos H. 'Balanced analgesia' in the perioperative period: is there a place for ketamine? Pain 2001;92:373-80.
18. Brinck EC, Tiippana E, Heesen M, et al. Perioperative intravenous ketamine for acute postoperative pain in adults. Cochrane Database Syst Rev 2018;12:CD012033.
19. Hamp T, Baron-Stefaniak J, Krammel M, et al. Effect of intravenous S-ketamine on the MAC of sevoflurane: a randomised, placebo-controlled, double-blinded clinical trial. Br J Anaesth 2018;121:1242-8.
20. Tu W, Yuan H, Zhang S, et al. Influence of anesthetic induction of propofol combined with esketamine on perioperative stress and inflammatory responses and postoperative cognition of elderly surgical patients. Am J Transl Res 2021;13:1701-9.
21. Jonkman K, van Rijnsoever E, Olofsen E, et al. Esketamine counters opioid-induced respiratory depression. Br J Anaesth 2018;120:1117-27.
22. Drugs and Lactation Database (LactMed). Bethesda (MD): National Library of Medicine (US), 2006.
23. LiverTox: Clinical and Research Information on Drug-Induced Liver Injury. Bethesda (MD): National Institute of Diabetes and Digestive and Kidney Diseases, 2012.
24. Manasco AT, Stephens RJ, Yaeger LH, et al. Ketamine sedation in mechanically ventilated patients: A systematic review and meta-analysis. J Crit Care 2020;56:80-8.
25. Reese JM, Sullivan VF, Boyer NL, et al. A Non-Comparative Prospective Pilot Study of Ketamine for Sedation in Adult Septic Shock. Mil Med 2018;183:e409-13.
26. Flinspach AN, Booke H, Zacharowski K, et al. High sedation needs of critically ill COVID-19 ARDS patients-A monocentric observational study. PLoS One 2021;16:e0253778.
27. Cohen CJ, Bean BP, Tsien RW. Maximal upstroke velocity as an index of available sodium conductance. Comparison of maximal upstroke velocity and voltage clamp measurements of sodium current in rabbit Purkinje fibers. Circ Res 1984;54:636-51.
28. Hara Y, Tamagawa M, Nakaya H. The effects of ketamine on conduction velocity and maximum rate of rise of action potential upstroke in guinea pig papillary muscles: comparison with quinidine. Anesth Analg 1994;79:687-93.
29. Park YM, Kang WC, Suh SY, et al. Early repolarization is associated with atrial and ventricular tachyarrhythmias in patients with acute ST elevation myocardial infarction undergoing primary percutaneous coronary intervention. Int J Cardiol 2014;176:327-32.
30. Shaw RM, Rudy Y. Electrophysiologic effects of acute myocardial ischemia: a theoretical study of altered cell excitability and action potential duration. Cardiovasc Res 1997;35:256-72.

31. Baker LC, London B, Choi BR, et al. Enhanced dispersion of repolarization and refractoriness in transgenic mouse hearts promotes reentrant ventricular tachycardia. Circ Res 2000;86:396-407.
32. Long J, Gao H, Li H, et al. The effects of different concentrations of dexmedetomidine on ventricular electrophysiological properties in isolated rabbits hearts. J Clin Anesthesiol 2015;31:1000-2.
33. Wang G, Dai D, Gao H, et al. Sevoflurane Alleviates Reperfusion Arrhythmia by Ameliorating TDR and MAPD90 in Isolated Rat Hearts after Ischemia-Reperfusion. Anesthesiol Res Pract 2019;2019:7910930.
34. Hashimoto M. Draft ICH guideline S7B: guideline on safety pharmacology studies for assessing the potential for delayed ventricular repolarization (QT interval prolongation) by human pharmaceuticals. Nihon Yakurigaku Zasshi 2003;121:377-83.
35. Hondeghem LM, Carlsson L, Duker G. Instability and triangulation of the action potential predict serious proarrhythmia, but action potential duration prolongation is antiarrhythmic. Circulation 2001;103:2004-13.
36. Wit AL, Rosen MR, Hoffman BF. Electrophysiology and pharmacology of cardiac arrhythmias. II. Relationship of normal and abnormal electrical activity of cardiac fibers to the genesis of arrhythmias. A Automaticity. Am Heart J 1974;88:515-24.
37. Jalife J, Antzelevitch C, Lamanna V, et al. Rate-dependent changes in excitability of depressed cardiac Purkinje fibers as a mechanism of intermittent bundle branch block. Circulation 1983;67:912-22.
38. Starmer CF. The cardiac vulnerable period and reentrant arrhythmias: targets of anti- and proarrhythmic processes. Pacing Clin Electrophysiol 1997;20:445-54.
39. King JH, Huang CL, Fraser JA. Determinants of myocardial conduction velocity: implications for arrhythmogenesis. Front Physiol 2013;4:154.
40. Burt JM, Massey KD, Minnich BN. Uncoupling of cardiac cells by fatty acids: structure-activity relationships. Am J Physiol 1991;260:C439-48.
41. Dhein S, Krüsemann K, Schaefer T. Effects of the gap junction uncoupler palmitoleic acid on the activation and repolarization wavefronts in isolated rabbit hearts. Br J Pharmacol 1999;128:1375-84.
42. Morley GE, Vaidya D, Samie FH, et al. Characterization of conduction in the ventricles of normal and heterozygous Cx43 knockout mice using optical mapping. J Cardiovasc Electrophysiol 1999;10:1361-75.
43. Sigtermans M, Dahan A, Mooren R, et al. S(+)-ketamine effect on experimental pain and cardiac output: a population pharmacokinetic-pharmacodynamic modeling study in healthy volunteers. Anesthesiology 2009;111:892-903.
44. Pratila MG, Pratilas V. Anesthetic agents and cardiac electromechanical activity. Anesthesiology 1978;49:338-60.
45. Givvimani S, Qipshidze N, Tyagi N, et al. Synergism between arrhythmia and hyperhomo-cysteinemia in structural heart disease. Int J Physiol Pathophysiol Pharmacol 2011;3:107-19.
46. Traber DL, Wilson RD, Priano LL. Blockade of the hypertensive response to ketamine. Anesth Analg 1970;49:420-6.
47. Jung I, Jung SH. Vasorelaxant mechanisms of ketamine in rabbit renal artery. Korean J Anesthesiol 2012;63:533-9.
48. Traber DL, Wilson RD, Priano LL. Differentiation of the cardiovascular effects of CI-581. Anesth Analg 1968;47:769-78.
49. Juang MS, Yonemura K, Morioka T, et al. Ketamine acts on the peripheral sympathetic nervous system of guinea pigs. Anesth Analg 1980;59:45-9.
50. Montel H, Starke K, Görlitz BD, et al. Animal experiments on the effect of ketamine on peripheral sympathetic nerves. Anaesthesist 1973;22:111-6.

Cite this article as: Cao Y, Song Y, Wang Z, Tang J, Yi J, Liu Y, An L, Pan Z, Gao H. Effects of different dosages esketamine on cardiac conduction and heterogeneity of Cx43: the epicardial mapping in guinea pigs. Ann Transl Med 2022;10(14):772. doi: 10.21037/atm-22-2614

